4E analyses of integration of microbial desalination cell, humidification-dehumidification and reverse osmosis desalination to produce sustainable freshwater based on solar and wind energies

Mohammad Hassan Khoshgoftarmanesh [a], Sepehr Davadgaran[b], Seyed Alireza Mousavi Rabeti[c] and Ana M Blanco-Marigorta[d]

[a] Energy, Environment and Biological Systems Research Lab (EEBRlab), Division of Thermal Sciences and Energy Systems, Department of Mechanical Engineering, Faculty of Technology & Engineering, University of Qom, Qom, Iran, m.khoshgoftar@qom.ac.ir, mh.khoshgoftar@gmail.com
[b] Energy, Environment and Biological Systems Research Lab (EEBRlab), Division of Thermal Sciences and Energy Systems, Department of Mechanical Engineering, Faculty of Technology & Engineering, University of Qom, Qom, Iran, sepehrdavadgaran@gmail.com
[c] Energy, Environment and Biological Systems Research Lab (EEBRlab), Division of Thermal Sciences and Energy Systems, Department of Mechanical Engineering, Faculty of Technology & Engineering, University of Qom, Qom, Iran, mousavi.sayed20@gmail.com
[d] Department of Process Engineering, Universidad de las Palmas de Gran Canaria, Las Palmas de Gran Canaria, Spain, anamaria.blanco@ulpgc.es

Abstract:

Over time, the water shortage crisis will have irreparable effects on the lives of many organisms, including humans. As a small contribution to alleviate the problem, the present work presents an innovative cogeneration system based on solar and wind renewable energies for sustainable production of freshwater, power, and wastewater treatment. To produce freshwater and treat wastewater in this system, the integration of a Microbial Desalination Cell with a Humidification-Dehumidification and Reverse Osmosis water desalination unit has been used. These systems obtain the required heat from solar energy to produce freshwater, and when solar radiation is unable to provide this heat, a hydrogen internal combustion engine driven with wind energy is used. Excess heat from the internal combustion engine is fed into the organic Rankine cycle with the working fluid R141B to generate power, to reduce the system waste heat and to increase the efficiency. To check the performance of the proposed system, energy, exergy, exergeoeconomic, and exergoenvironmental (4E) analyses have been carried out. The results of the analysis of the integrated system show that this system can produce 720 kW of electricity and 5.36 m^3/h of freshwater. The energy efficiency of the system is 22.09%, and its overall cost rate and overall environmental impact rate are 540.33 $/h and 17.37 Pts/h, respectively.

Keywords:

Microbial Desalination Cell (MDC); Humidification-Dehumidification (HDH); Hydrogen Internal Combustion Engine (HICE); Solar and wind energy; Cogeneration.

1. Introduction

In today's world, the crisis of freshwater scarcity has become one of the main problems that are exacerbated in many regions of the world due to the continuous reduction of water resources and population growth. According to the World Health Organization statistics [1], only 30,000 m^3 of freshwater worldwide are accessible for human use, and the largest amount of freshwater exists as precipitation and polar ice caps in the North and South Poles, which are difficult to access. Producing freshwater through various methods has been proposed as one of the effective solutions for the optimal management of water resources. One of these methods is the use of cogeneration cycles for producing freshwater, wastewater treatment, and power generation simultaneously. In these systems, it is possible to increase efficiency and benefit from water, energy, and environmental resources.

To increase the efficiency of these systems in freshwater production, the HDH (Humidification-dehumidification) system can be used. In this system, by using air humidification and passing this air through

 https://doi.org/10.52202/069564-0167

a cold surface, water humidity can be recovered and fresh water can be produced [2]. Due to the lack of need for external energy sources and simple operation, as well as the benefits of low maintenance and capital costs, HDH has been proposed as an efficient method in freshwater production [3]. In this regard, zubair et al [4]. have investigated that the HDH desalination system integrated with solar evacuated tubes, in various locations, can produce freshwater in the range of 16,430 to 19,445 l with costs ranging from 0.032 to 0.038 US$ per litter. Furthermore, Khoshgoftar Manesh et al [5]. proposed a cycle along with HDH for the production of power, hydrogen, hot water, and freshwater. Their results indicate that the energy and exergy efficiencies, as well as the overall annual cost and environmental impacts of the system, are 23.87%, 28.21%, 0.144 kWh/$, and 0.024 Pts/kWh, respectively. In addition, it is possible to simultaneously generate electrical power, remove salt from water, and treat wastewater using Microbial Desalination Cell (MDC) systems [6]. The features of MDC are perfectly aligned with our goals in freshwater cogeneration cycles, wastewater treatment, and power generation. Furthermore, to prevent energy loss and increase freshwater production, the integration of HDH technology with RO (Reverse Osmosis) is used. By integrating HDH and RO technologies, Ravajiri et al [7]. produced a total of 184.3 m^3/h of freshwater.

There are various methods available for recovering heat used in the freshwater production process. Khoshgoftar Manesh et al [8]. explored a recovering heat process for freshwater production in a proposed system based on an integrated solid oxide fuel cell-gas turbine-organic Rankine cycle-multi effect distillation system. The optimized hybrid system was capable of producing 5000 cubic meters of freshwater per day with five effects on MED-TVC. Various sources such as internal combustion engines, turbines, and solar panels are utilized for heat recovery. However, among them, heat recovery from internal combustion engines is one of the best methods for freshwater production processes, considering the simultaneous production of power and heat as well as the high rate of heat entry into the system by the engines [9]. In addition, various fuels such as gasoline, diesel, and hydrogen can be used in internal combustion engines [10]. The use of hydrogen in these engines results in minimal carbon dioxide emissions and minimizes its pollutants [11]. Furthermore, due to its high atomic energy, the use of hydrogen provides very high efficiency in heat recovery [12]. Nikitin et al [13]. used HICE (Hydrogen Internal Combustion Engine) in a multi-generation system based on solar and wind energy. The dynamic results of HICE have been reported in several different cities, showing an average return ranging from 21.82% to 24.76%.

In cogeneration systems, renewable energies such as solar and wind energy can be utilized. The addition of these renewable energies to cogeneration systems provides numerous benefits for the cycle [14]. One of the greatest benefits of using renewable energies in cogeneration systems is the reduction in production costs [15]. These types of energies are obtained directly from nature, and the costs of fuel, maintenance, and installation of power and heat generation systems from these energies are much lower [16]. Moreover, the use of these energies leads to a reduction in environmental impacts due to the decrease in greenhouse gas emissions [17]. Khoshgoftar Manesh et al [18]. investigated the most important renewable energy-based polygeneration systems for producing fresh water using thermal desalination and membrane processes. The most promising options include the integration of thermal and membrane desalination technologies such as Multi-Stage Flash (MSF), Multi-Effect Distillation (MED), Humidification-Dehumidification (HDH), and Reverse Osmosis (RO). makkeh et al [19]. in another study, investigated a combined system of solar collectors and wind turbines for generating power and freshwater. They reported that this configuration reduces the cost of freshwater production by up to 23%.

Studies indicate that the use of various water desalination methods is essential for mitigating the water scarcity crisis. On the other hand, given the limitations of each water desalination method, integrating different desalination techniques can be effective in improving the efficiency of desalination plants. In this regard, the present work proposes a co-generation system for desalination, power generation, and wastewater treatment based on solar and wind energy. In this system, the scenario of freshwater production is evaluated for the first time by integrating MDC-HDH-RO. Solar energy is utilized to provide the required heat for the system. During possible periods of radiation reduction or at night, an internal combustion engine based on hydrogen produces simultaneous power and heat. Reducing engine losses and recovering its heat is essential for increasing efficiency, and the presence of an Organic Rankine Cycle (ORC) can greatly address this issue. In the end, energy, exergy, economic, and environmental analyses have been utilized in the present study to analyze the efficiency of using such a system from various perspectives. The innovations involved in the present work are as follows:

- Integration of MDC-HDH-RO desalination systems has been utilized for freshwater production.
- A combination of solar and wind energy has been employed to minimize the system's emissions.
- A hydrogen-based internal combustion engine has been utilized to simultaneously generate power and heat.

2. System description

The present work proposes a cogeneration system based on solar and wind energy for freshwater production, power generation, and wastewater treatment in Tehran, Iran. Tehran city is located between 51 degrees 6 minutes to 51 degrees 38 minutes east longitude and 35 degrees 34 minutes to 35 degrees 51 minutes north latitude. The average wind speed and solar radiation in Tehran are 4.5 m/s and 514.05 W/m^2, respectively [20].

To produce freshwater in the current system, MDC-HDH-RO desalination units have been integrated. The saline water is initially introduced into the MDC and desalination using anion exchange membranes (AEM) and cation exchange membranes (CEM) as well as the potential difference between the cells. This process leads to the pre-treatment of wastewater and power generation while producing freshwater. The saline water, after the primary desalination by MDC, enters the Flat Plate Collectors (FPC) and receives the required heat before being directed to the HDH desalination unit for further freshwater production. In HDH, the air is humidified under standard environmental conditions and, as a result of a collision with hot water, heat, and mass transfer occur. Following this, some amount of saline water enters the air as humidity and is transferred to the dehumidifier, where it undergoes mass and heat transfer in the presence of freshwater, resulting in increased production of freshwater. RO integration has been utilized at the outlet of HDH to increase efficiency and further enhance freshwater production.

Because solar energy varies throughout the day and to ensure stable production of fresh water, the use of an internal combustion engine allows for heat recovery in the freshwater production system. To reduce the environmental impact of ICE, hydrogen fuel has been considered for this equipment, which is produced using a PEM electrolyzer.

The power consumption of the PEM electrolyzer is supplied using renewable wind energy. Furthermore, wind turbines are also used to supply the electricity required for RO. The remaining power produced by the wind turbines is injected into the grid.

Finally, to reduce the thermal losses of the studied system, the use of an organic Rankine cycle with R141B as the working fluid has been considered. The proposed system is shown in Fig. 1.

The following assumptions have been made for this system:

- The system has been analyzed in a steady-state condition.
- Changes in potential and kinetic energies are negligible.
- The temperature, pressure, and relative humidity of Tehran city are considered to be 25℃, 1.01 bar, and 30%, respectively.
- Heat losses have been disregarded in all heat exchangers and water desalination units.
- An isentropic efficiency of 85% is considered for the organic turbine and an isentropic efficiency of 80% is considered for the organic pump.
- An isentropic efficiency of 85% is assumed for the RO pump.
- The salinity concentration of the feedwater to the MDC is 35000 mg/l [6].
- Artificial wastewater containing 1000 mg/L of acetate has been used as the feed for the MDC [6].
- The HDH packings are made of polypropylene and have a specific surface area of 320 m^2/m^3 [21].
- Only variations in the air in the x-direction and variations in water in the z-direction have been considered in the HDH desalination process.
- The LTW77 wind turbine model with a capacity of 1 MW has been considered [21].
- The temperature and pressure in the PEM electrolyzer are assumed to be constant at 80 ℃ and 1 bar, respectively [22].
- The air-to-fuel ratio for the internal combustion engine has been considered to be 34.3 [23].
- A 4-cylinder inline internal combustion engine model has been considered.

https://doi.org/10.52202/069564-0167

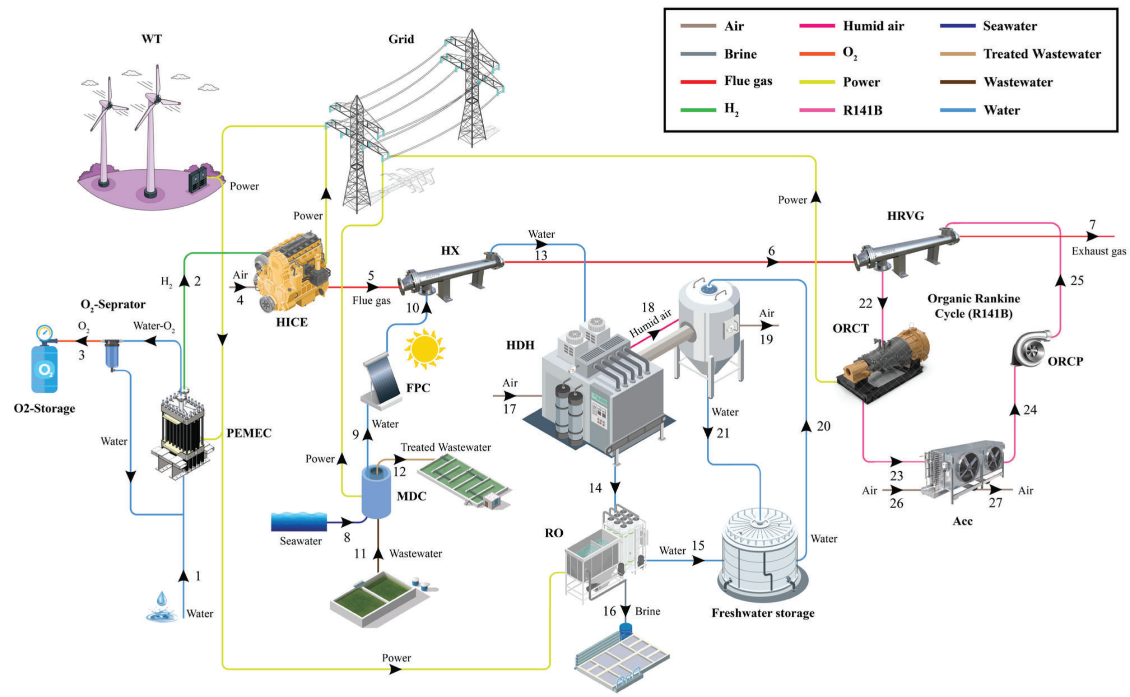

Figure. 1. Schematic of proposed cogeneration for production of desalination, power, and wastewater treatment based on solar and wind energy.

3. Governing equations

The mass and energy balance of equipment is generally calculated using the following equations [24]:

$$\sum_{i=0}^{n} m_{in} - \sum_{i=0}^{n} m_{out} = \left(\frac{dm}{dt}\right)_{system}, \tag{1}$$

$$\mathrm{Q} - \mathrm{W} + \sum_{i=0}^{n} \mathrm{m_{in}} \left(\mathrm{h} + \frac{\mathrm{V}^2}{2} + \mathrm{gz}\right)_{\mathrm{in}} - \sum_{i=0}^{n} \mathrm{m_{out}} \left(\mathrm{h} + \frac{\mathrm{V}^2}{2} + \mathrm{gz}\right)_{\mathrm{out}} = \left(\frac{\mathrm{dE}}{\mathrm{dt}}\right)_{\mathrm{system}}, \tag{2}$$

The concepts of m which means mass flow rate, Q which means heat transfer, and W which means exchanged power is used in the above equation. In Equation 2, the terms within the summation represent the energy flows at the inlet and outlet of the control volume, associated with the energy of the flows. Terms containing V or Z are considered to be zero due to neglecting the kinetic and potential energies. Also, h represents the specific enthalpy. It should be noted that for open systems operating under steady-state conditions, Equations 1 and 2 can be defined in the following form: d/dt=0. However, in many pieces of equipment, it is necessary to create equations to improve their modelling. For example, for flat plate solar collectors, their specific surface area for absorbing solar energy needs to be calculated. Therefore, the heat transfer equations related to this type of equipment should be considered [25]. Moreover, for modelling a PEM electrolyzer, it is necessary to calculate the power consumption by specifying the produced hydrogen flow rate and the potential equations of this electrolyzer [22]. Modelling an RO desalination system requires taking into account the equations related to osmotic and mechanical pressure. Then, the amount of produced freshwater and the pump power consumption of the RO system can be calculated through the recovery ratio [26]. Continuing, for modelling an internal combustion engine based on hydrogen, the amount of recovered heat is calculated by knowing the engine's nominal power [27, 28]. Additionally, to model a wind turbine based on the wind speed of the study area, the equations presented in the references [19, 29] have been used. To model an MDC system, the differential equations presented in the reference [6] have been used. These equations consist of mass balance equations for substrate and microorganisms in the anode compartment, mass balance equations for salt in the desalination compartment, anode compartment, and cathode compartment, in addition to equations for the current generation, which all must be solved simultaneously. The MDC inputs have been obtained from the references [6, 30]. The differential equations for modelling HDH consist of heat and mass transfer equations for water and air in the dehumidifier and humidifier [31]. These equations must also be solved simultaneously.

It is not entirely possible to assess the quality of energy processes in terms of reversibility. Therefore, by adding the concept of exergy to energy analysis, a more comprehensive view of entropy generation and evaluation of the irreversibility of energy processes can be obtained. Thus, exergy is defined as the useful work capacity and its calculation is relative to a dead reference. The overall exergy balance for all energy systems operating in steady-state can be defined by the following equation [32]:

$$E\,x_Q - E\,x_W + \sum_{i=1}^{n} E\,x_{in} - \sum_{i=1}^{n} E\,x_{out} + E\,x_D = 0, \quad (3)$$

In the above equations, Ex_Q refers to thermal exergy, Ex_W refers to power exergy, and Ex_D refers to the destruction of exergy, which is created as a result of entropy production. The expressions within the summation sign correspond to the flow exergy at the input and output of exergy systems.

Given that the capital payback period and profitability are crucial in system planning, after examining the energy aspects of the system, its economic aspects should also be considered. The economic balance of steady-state energy systems with an exergy approach is defined as follows [33]:

$$C_Q - C_w + \sum_{i=1}^{n} C_{in} \sum_{i=0}^{n} C_{out} + Z_k = 0, \quad (4)$$

In the above equations, C_Q means the heat cost, C_W means the power cost, and Z_k means the equipment purchase rate of the energy system, which is calculated based on references [21, 33].

Life cycle assessment (LCA) is a method for evaluating the environmental pollutants released during the life cycle of a system, from raw material extraction to transportation, construction, and disposal. In the current research, environmental analysis based on LCA, which is defined based on exergy analysis, has been used. Environmental balance is defined for systems operating in a steady state as follows [33]:

$$B_Q - B_w + \sum_{i=1}^{n} B_{in} \sum_{i=0}^{n} B_{out} + Y_k = 0, \quad (5)$$

In the above equations, B_Q means the environmental impact of heat, B_W means the environmental impact of power, and Y_k means the rate of environmental impacts of energy system equipment, which can be calculated using the equations from references [5, 33]. In addition, the constants used in this study are as follows: a 10% interest rate, a maintenance factor of 1.06, a 20-year lifespan for the power plant, 3500 operating hours for FPC, 6000 operating hours for WT, and 8000 operating hours for other equipment [33]. It should be noted that for economic and environmental calculations, the investment cost and equipment weights were obtained from references [5, 21].

4. Results

Table 1 shows the extent of the exergy destruction, costs, destruction costs, environmental impacts, and environmental destruction effects associated with each piece of equipment used in the proposed system. The results of this section indicate that exergy destruction in wind turbines is higher than in other equipment in the system. The reason for this is the higher power production in wind turbines compared to other equipment in the system. After the wind turbine, the internal combustion engine has the highest exergy destruction due to irreversibilities and chemical reactions within it. Regarding the cost destruction, it should be noted that the cost destruction associated with the internal combustion engine is calculated to be higher than other equipment due to the chemical reactions occurring within it. After the internal combustion engine, the PEM electrolyzer has the highest cost destruction. Systems that operate with renewable energy sources (WT, FPC, MDC) have no cost destruction. The results regarding environmental degradation are similar, with the difference that the heat exchanger after the internal combustion engine has the highest environmental degradation.

In Table 2, the results of the 4E analysis of the proposed system are presented. Based on these results, the net power generation, cogeneration exergy efficiency, overall cost rate, and overall environmental impact rate of the system are 0.72 MW, 4.55%, 540.33 $/h, and 17.37 Pts/h, respectively.

Fig. 2 represents the change in humid air temperature inside HDH desalination. In Fig. 2(a), temperature changes in humidification are shown. As expected, the air in contact with warmer saltwater gets hotter. The modelling results also demonstrate these temperature changes with an increase in the length of humidification. In Fig. 2(b) as well, these changes are shown for dehumidification, which operates in reverse. That means the temperature of the humid air decreases in the vicinity of cooler freshwater. These results are also consistent with the modelling.

Fig. 3 shows the absolute humidity change of the air in the HDH desalination. The results of Fig. 3(a) indicate that after the air enters the device, it interacts with salty water and its absolute humidity increases. This result is consistent with the modelling. On the other hand, in Fig. 3(b), in the dehumidification process, water is absorbed from the air, which causes the air to become drier and its absolute humidity to decrease. This process, due to mass transfer with water, leads to the production of freshwater.

https://doi.org/10.52202/069564-0167

Table 1. The main result of exergy, exergoeconomic, and exergoenvironmental analysis for all components of the proposed system

Component	$\dot{E}x_D\ (MW)$	$\dot{Z}\left(\frac{\$}{h}\right)$	$\dot{C}_D\left(\frac{\$}{h}\right)$	$\dot{Y}\left(\frac{mPts}{h}\right)$	$\dot{B}_D\left(\frac{mPts}{h}\right)$
WT	10.25	378.40	0.00	16647.37	0.00
PEMEC	2.84	123.69	133.54	80.92	5875.12
HICE	5.11	5.98	424.39	2.06	14091.21
Hx	0.03	0.07	17.97	0.05	5897.87
HRVG	0.08	0.34	53.82	0.20	1765.90
ORCT	0.01	0.62	16.08	406.27	178.47
ACC	0.02	0.04	--	0.00	--
ORCP	0.00	0.01	0.60	0.01	21.61
MDC	0.22	0.02	0.00	63.84	0.00
FPC	0.99	15.28	0.00	16.77	0.00
HDH	0.02	1.25	25.13	0.00	491.53
RO	0.01	14.65	8.85	149.62	178.47

Table 2. Overall results of the analysis.

Parameters	value
Net power generation (MW)	0.72
Total freshwater production (m^3/h)	5.36
Cogeneration energy efficiency (%)	22.09
Total exergy destruction (MW)	18.73
Cogeneration exergy efficiency (%)	4.55
Overall cost rate ($/h)	540.33
Overall environmental impact rate (Pts/h)	17.37
Levelized cost of electricity ($/kWh)	0.75
Levelized environmental impact of electricity (Pts/kWh)	0.02
Number of wind turbine	23
Solar field area (m^2)	3000

Fig. 4 shows the change in water temperature in the HDH desalination. In humidification, considering that the incoming water has a higher temperature than the air, it is expected that due to the heat and mass transfer, the temperature of the outlet water is lower. This expectation is consistent with the results of the modelling shown in Fig. 4(a). In this plot, as we move upwards, the water temperature decreases. In dehumidification, conversely, humid air interacts with sweet water and causes the outlet water to become warmer. Therefore, it is expected that the outlet water has a higher temperature than the incoming water. This expectation is consistent with the Fig. 4(b) plot, in a way that as we move upwards in the plot, the water temperature increases.

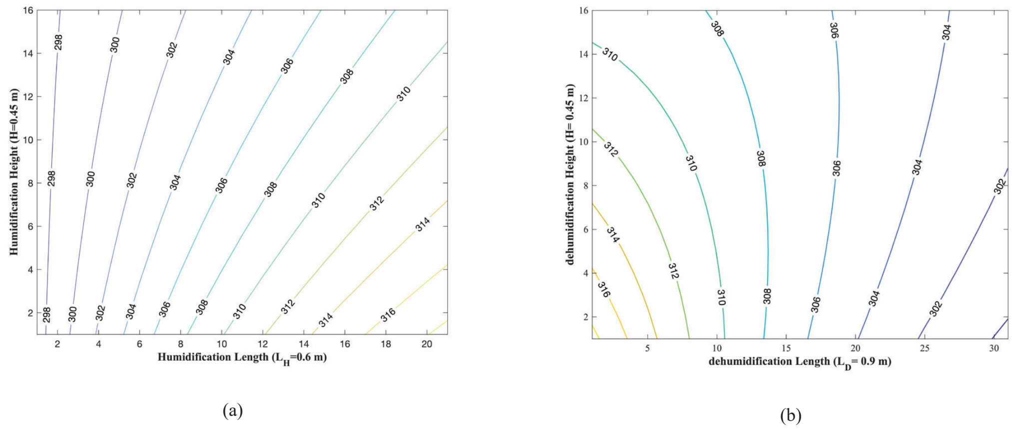

Figure. 2. Humid air temperature change in HDH Desalination.

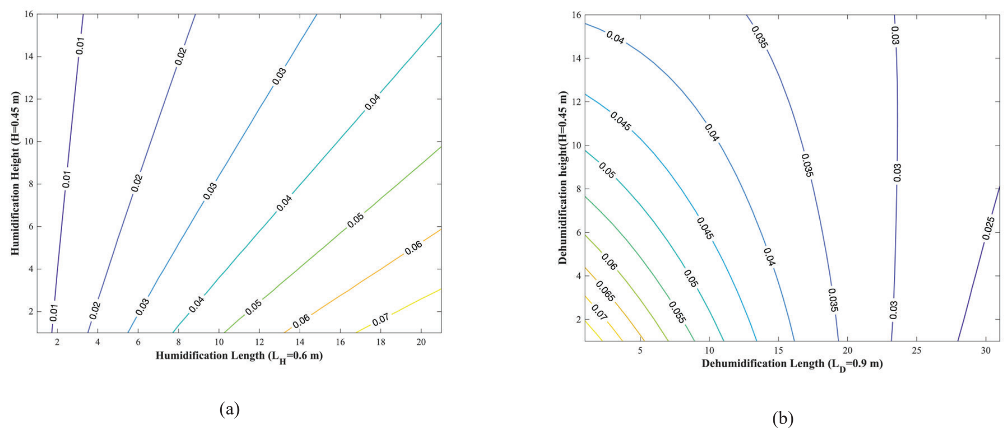

Figure. 3. Absolute humidity change in HDH Desalination.

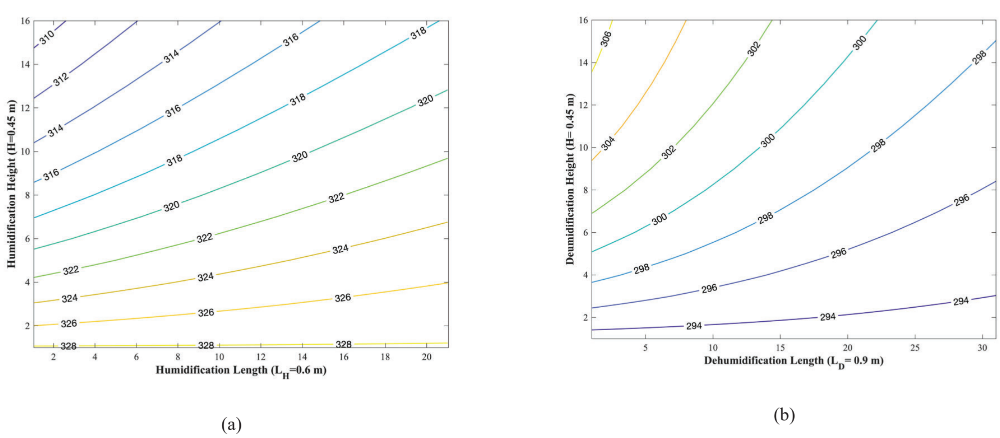

Figure. 4. Water temperature change in HDH Desalination.

https://doi.org/10.52202/069564-0167

Fig. 5 illustrates the change in water mass flow rate in HDH desalination. In humidification, the water mass flow rate decreases and is added to the ambient air humidity, which its variations are observable. In other words, as we move upwards in plot Fig. 5(a), the water mass flow rate decreases, and the humidity of the ambient air increases. In Fig. 5(b), these changes can be observed conversely for dehumidification.

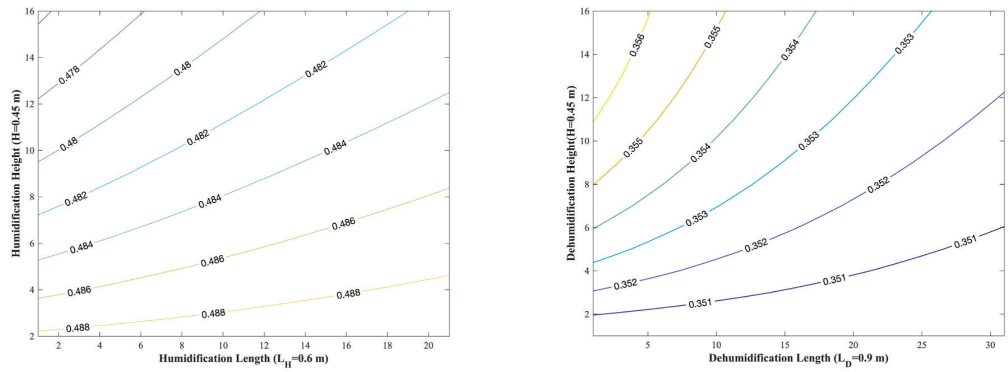

(a) (b)

Figure. 5. Specific water mass flow rate change in HDH Desalination.

Fig. 6(a) displays the changes in salt concentration over time in the intermediate chamber for different initial salt concentrations. The results indicate that for the initial salt concentration of 35g/l, desalination was achieved by a considerable amount of 65.85%. In Fig. 6(b), the effect of changes in the salt solution flow rates on the variation of salt concentration in the intermediate chamber has been investigated. The results indicate that a higher percentage of desalination can be achieved by decreasing the salt solution flow rates. In other words, desalination has increased from 19.28% at a flow rate of 20 l/day to 77.82% at a flow rate of 0.05 l/day.

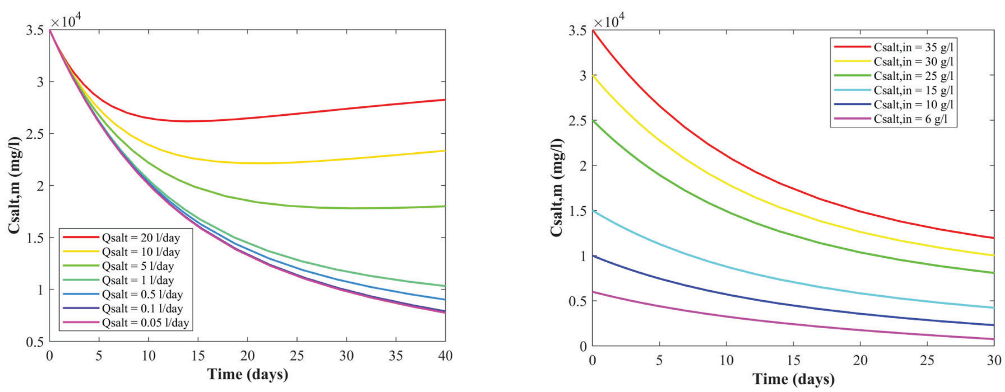

(a) (b)

Figure. 6. The salt concentration in the desalination compartment with time for (a) different salt solution flow rates, (b) different initial salt concentrations (when Q_{salt} = 0.1 l/day).

Fig. 7 illustrates that as the growth rate of methanogenic bacteria increases, the current generation decreases and ultimately experiences maximum enhancement when the rate of methanogenic production is equal to zero. Thus, the results confirm that methanogenic bacteria lead to a reduction in the current generation.

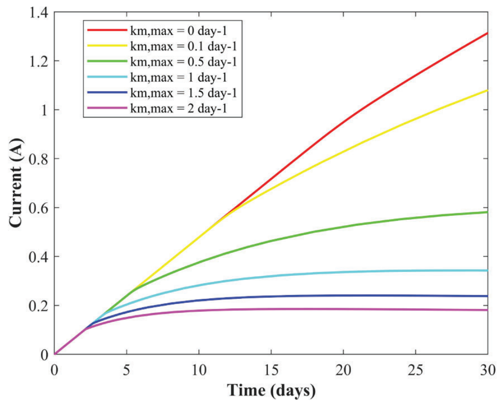

Figure. 7. The relationship between the current production and methanogenic growth rate.

5. Conclusions

The present work presented a cogeneration system for the production of power, freshwater, and wastewater treatment based on solar and wind energy. For freshwater production, the integration of MDC with HDH and RO systems was investigated. The required heat of the complex was combined using FPC and HICE based on solar and wind energy. Energy, exergy, exergeoeconomic, and exergoenvironmental (4E) analyses were used for the integrated system. The overall results obtained indicate that the integrated system can produce 0.72 MW power and 5.36 m^3/h freshwater. Also, the overall cost rate and overall environmental impact rate of the whole system were calculated as 540.33 $/h and 17.37 Pts/h, respectively. A series of other results of the system are as follows:

- In addition to wastewater treatment and power production, the MDC has been able to reduce the concentration of dissolved salt in water by 20 g/kg.
- The RO desalination plant has produced 1.42 kg/s of freshwater using 6 kW of power.
- The highest exergy destruction is related to WT and HICE, respectively.
- The most destructive of costs and destruction of environmental impacts are related to HICE.
- WT has the highest production environmental impacts and the highest investment cost.

In the end, it should be mentioned that the presented system can be used to meet the needs of greenhouses, industrial factories, residential areas, and military barracks. But it is necessary to examine the feasibility of using such a system from various aspects such as safety risk, controllability, etc.

Acknowledgments

This research has been co-funded by ERDF funds, INTERREG MAC 2014-2020 programme, within the E5DES project (MAC2/1.1a/309). No funding sources had any influence on study design, collection, analysis, or interpretation of data, manuscript preparation, or the decision to submit for publication.

References

[1] Invest in climate action for health: cut emissions, clean our air, save lives. World Health Organization. Available at: <https://www.who.int/director-general/speeches/detail/invest-in-climate-action-for-health-cut-emissions-clean-our-air-save-lives> [accessed 23.9.2019].

[2] Jamil, M. A., Elmutasim, S. M., & Zubair, S. M. Exergo-economic analysis of a hybrid humidification dehumidification reverse osmosis (HDH-RO) system operating under different retrofits. Energy Conversion and Management 2018; 158, 286-297.

[3] Ding, P., Yuan, Z., Shen, H., Qi, H., Yuan, Y., Wang, X., ... & Sobhani, B. Exergoeconomic analysis and optimization of a hybrid Kalina and humidification-dehumidification system for waste heat recovery of low-temperature Diesel engine. Desalination 2020; 496, 114725.

[4] Zubair, M. I., Al-Sulaiman, F. A., Antar, M. A., Al-Dini, S. A., & Ibrahim, N. I. Performance and cost assessment of solar driven humidification dehumidification desalination system. Energy Conversion and Management 2017; 132, 28-39.

[5] Manesh, M. K., Rabeti, S. M., Nourpour, M., & Said, Z. J. S. E. T. Energy, exergy, exergoeconomic, and exergoenvironmental analysis of an innovative solar-geothermal-gas driven polygeneration system for

 https://doi.org/10.52202/069564-0167

combined power, hydrogen, hot water, and freshwater production. Sustainable Energy Technologies and Assessments 2022; 51, 101861.

[6] Khaled, H., Zrelli, A., Hamed, M., & Chaouachi, B. Modelisation and Optimization of a Microbial Desalination Cell System. Journal of Sustainable Bioenergy Systems 2021; 11(3), 118-130.

[7] Ravajiri, E. S., Jalali, A., & Houshfar, E. Multi-objective optimization and 4E analysis of an integrated system based on waste-to-energy, solar PV, power-to-gas, and HDH-RO desalination. Energy Conversion and Management 2023; 277, 116677.

[8] Manesh, M. H. K., Ghorbani, S., & Blanco-Marigorta, A. M. Optimal design and analysis of a combined freshwater-power generation system based on integrated solid oxide fuel cell-gas turbine-organic Rankine cycle-multi effect distillation system. Applied Thermal Engineering 2022; 211, 118438.

[9] Reitz, R. D., Ogawa, H., Payri, R., Fansler, T., Kokjohn, S., Moriyoshi, Y., ... & Zhao, H. IJER editorial: The future of the internal combustion engine. International Journal of Engine Research 2019; 21(1), 3-10.

[10] Martins, J., & Brito, F. P. Alternative fuels for internal combustion engines. Energies 2020; 13(16), 4086.

[11] Shadidi, B., Najafi, G., & Yusaf, T. A review of hydrogen as a fuel in internal combustion engines. Energies 2021; 14(19), 6209.

[12] Tsujimura, T., & Suzuki, Y. The utilization of hydrogen in hydrogen/diesel dual fuel engine. International journal of hydrogen energy 2017; 42(19), 14019-14029.

[13] Nikitin, A., Deymi-Dashtebayaz, M., Baranov, I. V., Sami, S., Nikitina, V., Abadi, M. K., & Rumiantceva, O. Energy, exergy, economic and environmental (4E) analysis using a renewable multi-generation system in a near-zero energy building with hot water and hydrogen storage systems. Journal of Energy Storage 2023; 62, 106794.

[14] He, Y., Guo, S., Zhou, J., Wu, F., Huang, J., & Pei, H. The many-objective optimal design of renewable energy cogeneration system. Energy 2021; 234, 121244.

[15] Brown, M. A., & Herrera, V. S. Combined heat and power as a platform for clean energy systems. Applied Energy 2021; 304, 117686.

[16] Gonzalez, A., Riba, J. R., Esteban, B., & Rius, A. Environmental and cost optimal design of a biomass–Wind–PV electricity generation system. Renewable energy 2017; 126, 420-430.

[17] Zhao, Z. Y., Chen, Y. L., & Thomson, J. D. Levelized cost of energy modeling for concentrated solar power projects: A China study. Energy 2017; 120, 117-127.

[18] Khoshgoftar Manesh, M. H., & Onishi, V. C. Energy, exergy, and thermo-economic analysis of renewable energy-driven polygeneration systems for sustainable desalination. Processes 2021; 9(2), 210.

[19] Makkeh, S. A., Ahmadi, A., Esmaeilion, F., & Ehyaei, M. A. Energy, exergy and exergoeconomic optimization of a cogeneration system integrated with parabolic trough collector-wind turbine with desalination. Journal of Cleaner Production 2020; 273, 123122.

[20] Alamdari, P., Nematollahi, O., & Mirhosseini, M. Assessment of wind energy in Iran: A review. Renewable and Sustainable Energy Reviews 2012; 16(1), 836-860.

[21] Khani, N., Manesh, M. H. K., & Onishi, V. C. 6E analyses of a new solar energy-driven polygeneration system integrating CO2 capture, organic Rankine cycle, and humidification-dehumidification desalination. Journal of Cleaner Production 2022; 379, 134478.

[22] Ahmadi, P., Dincer, I., & Rosen, M. A. Energy and exergy analyses of hydrogen production via solar-boosted ocean thermal energy conversion and PEM electrolysis. International Journal of Hydrogen Energy 2013; 38(4), 1795-1805.

[23] Akal, D., Öztuna, S., & Büyükakın, M. K. A review of hydrogen usage in internal combustion engines (gasoline-Lpg-diesel) from combustion performance aspect. International journal of hydrogen energy 2020; 45(60), 35257-35268.

[24] Cengel, Y. A., Boles, M. A., & Kanoğlu, M. Thermodynamics: an engineering approach New York: McGraw-hill; 2011.

[25] Bellos, E., & Tzivanidis, C. Performance analysis and optimization of an absorption chiller driven by nanofluid based solar flat plate collector. Journal of cleaner production 2018; 174, 256-272.

[26] Zhou, W., Song, L., & Guan, T. K. A numerical study on concentration polarization and system performance of spiral wound RO membrane modules. Journal of Membrane Science 2006; 271(1-2), 38-46.

[27] Wang, J., Wu, J., & Wang, H. Experimental investigation of a dual-source powered absorption chiller based on gas engine waste heat and solar thermal energy. Energy 2015; 88, 680-689.

[28] Norani, M., & Deymi-Dashtebayaz, M. Energy, exergy and exergoeconomic optimization of a proposed CCHP configuration under two different operating scenarios in a data center: Case study. Journal of Cleaner Production 2022; 342, 130971.

[29] Rokni, M. M. Power to hydrogen through polygeneration systems based on solid oxide cell systems. Energies 2019; 12(24), 4793.

[30] Pinto, R. P., Srinivasan, B., Manuel, M. F., & Tartakovsky, B. A two-population bio-electrochemical model of a microbial fuel cell. Bioresource technology 2010; 101(14), 5256-5265.

[31] Zamen, M., Amidpour, M., & Firoozjaei, M. R. A novel integrated system for fresh water production in greenhouse: Dynamic simulation. Desalination 2013; 322, 52-59.

[32] Dincer, I., Rosen, M. A., & Ahmadi, P. Optimization of energy systems. John Wiley & Sons; 2017.

[33] Cavalcanti, E. J. C. Exergoeconomic and exergoenvironmental analyses of an integrated solar combined cycle system. Renewable and Sustainable Energy Reviews 2017; 67, 507-519.

 https://doi.org/10.52202/069564-0167